Running title: Burst Ensemble Multiplexing

Full title: Burst Ensemble Multiplexing: A Neural Code Connecting Dendritic Spikes with Microcircuits

Authors: Richard Naud[1,2] and Henning Sprekeler[2]

Affiliations: 1:Brain and Mind Research Institute, Department of Cellular and Molecular Medicine, University of Ottawa, 451 Smyth Rd, K1H 8M5 Ottawa, Canada. 2: Bernstein Center for Computational Neuroscience Berlin, Technische Universität Berlin, Marchstr 23, 10587 Berlin, Germany.

Corresponding Author:
Richard Naud
Department of Cellular and Molecular Medicine
University of Ottawa
451 Smyth Rd, K1H 8M5
Ottawa, Canada
Ph. (613) 778-8050

Acknowledgments: We thank Guillaume Hennequin, Jean-Claude Béïque, Albert Gidon and Matthew Larkum for helpful discussions. We thank Loreen Hertäg, Alexandre Payeur and Stephen E. Clarke for critical reading of the manuscript as well as Greg Knoll for an independent verification of the numerical results. This work was supported by a Bernstein Award (01GQ1201) by the German Federal Ministry for Science and Education and an NSERC Discovery Grant 06872. Part of this work was conducted (RN and HS) at the Computational and Biological Learning Laboratory, Department of Engineering, University of Cambridge, UK.

Author Declarations: The authors declare no conflict of interest.

Keywords: neural coding |cerebral cortex | bursting | multiplexing | decoding | spike timing | short-term plasticity

Author Contributions: HS and RN designed the study and wrote the manuscript. RN performed the simulations analyzed the results and carried out the theoretical analysis.

Abstract

Thick-tufted pyramidal neurons of the neocortex (TPNs) receive distinct types of inputs onto different parts of their dendritic arborization. In the classical view, these distinct inputs are combined nonlinearly to give rise to a single firing rate output, which collapses all input streams into one. Here, we propose an alternative view, in which a single neural ensemble can represent both a somatic/proximal and a dendritic/distal input stream simultaneously, by using a multiplexed code that distinguishes single spikes and bursts of action potentials. Using computational simulations constrained by experimental data, we first show that the electrophysiological properties of TPNs are well suited to generate such a multiplexed neural code. Secondly, an information theoretical analysis shows that this novel neural code maximizes information for short and sparse bursts, consistent with in vivo recordings. Finally, we show that the two inputs streams can be decoded by widespread neural microcircuits, which combine short-term plasticity with feedforward inhibition. We propose that multiplexed temporal codes could be advantageous throughout the nervous system because they offer the opportunity for downstream neurons to flexibly interpret multiple streams of information.

Introduction

Cracking the neural code is to attribute proper meaning to temporal sequences of action potentials. Important clues to this riddle are the biophysical mechanisms that mediate the encoding and decoding of information in spike trains. For instance, shared afferents allow populations of neurons to encode information in the temporal variations of the ensemble-averaged firing rate[1]. Downstream neurons can easily decode this firing rate by summing spikes from its synaptic afferents. Other biophysical mechanisms – feedback inhibition[2–5], adaptation[6] – are thought to support and optimize this firing rate code. Additional support for a given coding strategy can be gathered by showing that it alleviates an evolutionary pressure. For instance, ensemble rate coding satisfies the need for fast information processing[7], since encoding and decoding can be performed in a few milliseconds[1,8]. Yet, in theory, spike trains contain significantly more information than what is recovered from the firing rate alone[9,10]. Neurons could convey additional information using spike-timing patterns, the phase of spikes relative to ongoing oscillations, or potentially other neural codes (reviewed in[1,11]). How this additional information is encoded and decoded with the biophysical mechanisms in place remains to be fully articulated.

One simple way to extract more information from spike trains is to classify two types of spike-timing patterns, one that consists of a stereotypical burst of spikes in close succession, and one that consists of a single spike in relative isolation. What is the proper meaning of these spike timing patterns? Again, the underlying mechanisms could provide clues. In the cortex, a well-studied biophysical mechanism for generating bursts hinges on voltage-dependent activation of ion channels in the apical dendrite[12–14]. Unlike many other mechanisms[15] that alternate burst and quiescence, dendrite-dependent bursting allows a mixture of single spikes and bursts. This modulation of the spike timing structure is likely to depend on the proportion of input impinging the distal dendrites[16,17]. Interestingly, proximal and distal dendrites of pyramidal cells often receive inputs of a distinct nature in the neocortex[12,18–20] and in the hippocampus[21,22]. Hence, dendritic nonlinearities, in addition to enhancing the computational power of single neurons[23–26], could play a role in encoding different information streams in distinct spike-timing patterns.

Consistently, specific biophysical mechanisms appear well-suited to read a burst code: short-term synaptic facilitation (STF) enhances the post-synaptic effect of bursts, whereas short-term depression (STD) decreases the post-synaptic effect of secondary spikes within a burst[27–29]. Since the same axon will produce either STF or STD depending on the post-synaptic target[27,30], short-term plasticity (STP) can use spike-timing patterns to separate different streams

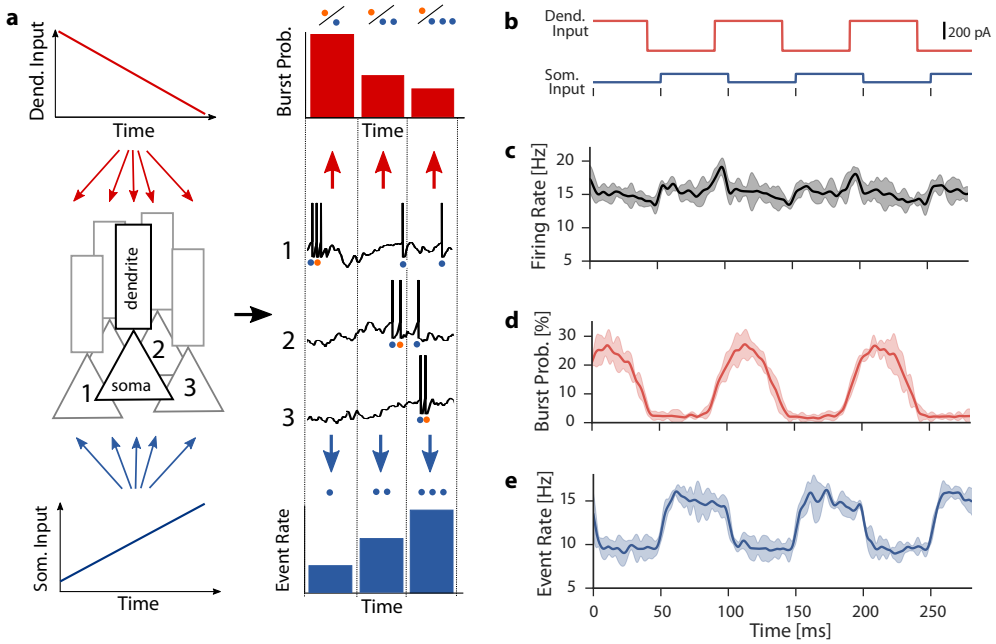

Figure 1 Burst ensemble multiplexing for representing two streams of information simultaneously. **a** Schema of the suggested neural code: Two input streams are delivered to the somata and dendrites of a neural ensemble. Each neuron responds with a series of action potentials (black traces), which can be classified as isolated spike events or burst events on the basis of the interspike interval. The total number of events (blue dots) can be computed in each time bin to form an event rate (blue bars). The burst probability (red bars) is calculated by taking the ratio of the number of bursts (orange dots) and the total number of events for each time step. **b-e** Multiplexing somatic and dendritic input signals: **b** Alternating somatic and dendritic input currents were used as inputs to a population of 4 000 two-compartment neuron models. Phase lag and amplitudes were chosen such that **c** the output firing rate remains largely constant, to illustrate the ambiguity of the firing rate code. **d** The ensemble burst probability reflects the alternating dendritic input. **e** The ensemble event rate reflects the alternating somatic input. Shaded regions show one standard deviation calculated from 5 trials.

post-synaptically. It is not clear, however, how and to what extent the short and sparse bursts observed in vivo[31,32] can be processed by STF and STD alone[33]. Yet, a potential player, whose role in this computation has attracted much less attention, could be the interconnection motifs observed between different neocortical cell types[34,35].

Here we advocate that i) neural ensembles multiplex information coming from distinct input streams in the *ensemble average* of different spike timing-patterns and that ii) short-term plasticity (STP) in microcircuits is tuned to support this multiplexing. Using computer simulations based on experimentally-calibrated cellular and synaptic models[36,37], we show that the biophysics of Thick-tufted Pyramidal Neuron (TPN) ensembles preserve information specific to inputs to the proximal or apical dendrites. We then derive an expression for the mutual information between the input and the output of the ensemble and show that information transmission is maximized for short and sparse bursts. Furthermore, we demonstrate that STP within a common cortical microcircuit is consistent with a demultiplexing of this information. To illustrate a novel computation on this multiplexed neural code, we show that dendritic feedback inhibition combined with demultiplexing microcircuits can be used to optimize information transmission. These results offer a novel view on the neural code and how cortical networks process information. We argue that burst ensemble multiplexing (BEM) satisfies the need to rapidly, flexibly and unambiguously combine external and internal information.

Results

We consider a neural code where spike-timing patterns – single spikes and bursts – are separated at the level of individual spike trains before being averaged across a neural ensemble (Fig. 1a), yielding time-varying rates of single spikes and bursts, respectively. How could these two rates represent different input streams? The simpler variant would be that single spikes and bursts are generated by two independent cellular mechanisms that each depend on one input stream alone. In this case, the ensemble singlet rate and ensemble burst rate would encode these streams independently. Alternatively, bursts could be generated by a synergy of the two input streams. In this case, both singlet rate and burst rate represent a mixture of the two input streams. Of these two variants, many mechanisms of burst generation[12,13,38–40] suggest the latter. In TPNs, dendritic spikes convert a somatically induced singlet into a burst under the condition of potent distal dendritic input[12]. Therefore, we reason that, in TPNs, a dendritic input stream is encoded in the probability that a somatically induced spike is converted into a burst. This *burst probability*[41] is reflected by the fraction of active cells that emit a burst (Fig. 1a). Then, a somatic input stream should be reflected in rate of events, that is either a singlet or a burst. We termed this quantity *event rate* (Fig. 1a) and it is calculated by taking the sum of the singlet rate and the burst rate. In the following, we use computational modeling and theoretical analyses to ask whether the anatomy and the known physiology of the neocortical networks is consistent with this neural code.

Encoding: BAC-firing as a Multiplexer

To illustrate BEM in cortical ensembles, we first consider the firing statistics of model TPNs as they respond to alternating dendritic and somatic input shared among neurons (Fig. 1b). Individual TPNs are simulated using a two-compartment model that has been constrained by electrophysiological recordings to capture dendrite-dependent bursting (Fig. S1a-d[12]), a critical frequency for somatic stimulation (Fig. S1e-h[42]), and the spiking response of TPNs to complex stimuli *in vitro*[36]. In addition to the shared alternating signals, each cell in the population receives independent background noise to reproduce the high variability of recurrent excitatory networks balanced by inhibition, as well as low burst fraction and the typical membrane potential standard deviation observed in vivo[5,32,43] (see

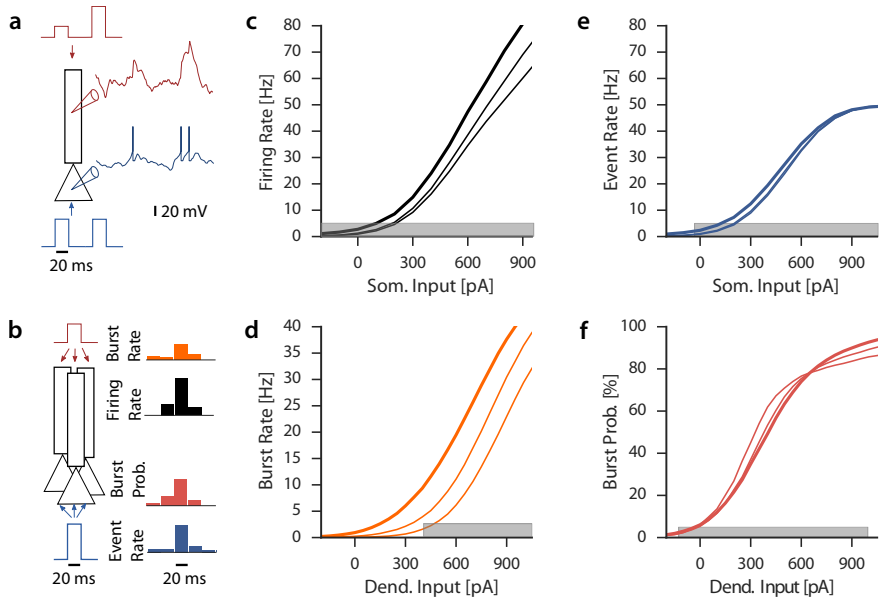

Figure 2 Input-output functions for distinct spike-timing patterns reveal a large multiplexing range. **a** The two-compartment TPN model combines background noise with dendrite-dependent burst firing in the presence of high somatic and dendritic inputs. **b** I-O functions are computed by simulating the response of 4000 TPNs to short current pulses and averaging across the ensemble. **c** The ensemble firing rate as a function of the somatic input amplitude is shown in the presence of a concomitant dendritic input (0, 200, 400 pA, thicker line corresponds to larger dendritic input). **d** The ensemble burst rate as a function of the dendritic input amplitude is shown in the presence of concomitant somatic input pulses (0, 200, 400 pA, thicker line corresponds to greater somatic input). **e** Same as **c** but for the ensemble event rate. **f** Same as **d** but for the burst probability, computed by dividing the ensemble burst rate with the event rate. Gray bars indicate the input regimes associated with SNR_I>1 (see SI Data Analysis Methods).

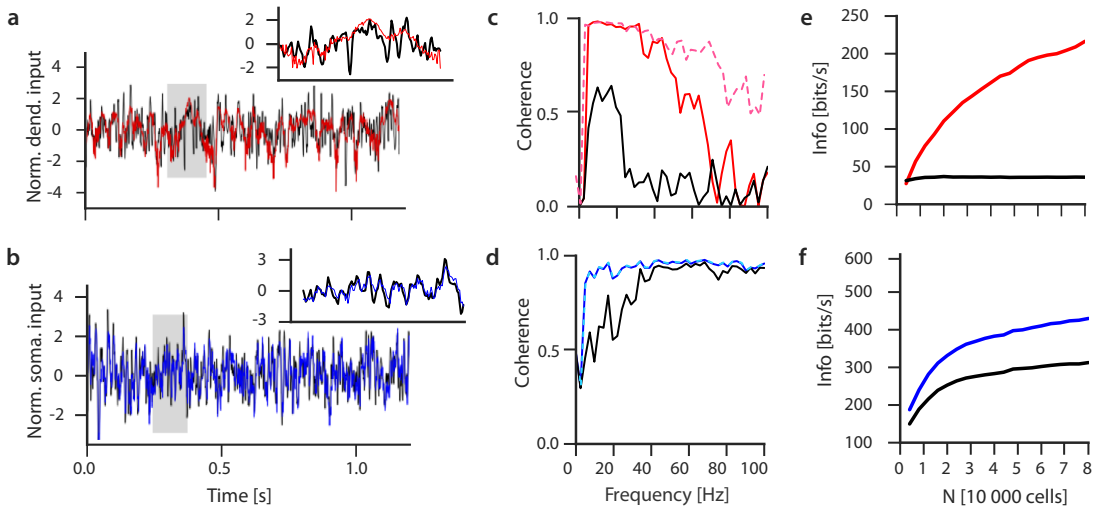

Figure 3 Decoding multiplexed time-dependent information. **a** The logarithm of the burst probability (red, normalized) is used as a decoded estimate of the dendritic input current (black, normalized). Inset: Blow-up of the shaded region. **b** The logarithm of the event rate (blue, normalized) is used as a decoded estimate of the somatic input current (black, normalized). Here, decoding is performed on an ensemble of 80,000 cells. **c** Coherence between dendritic input and the logarithm of the burst probability (red) or the logarithm of the firing rate (black). The bandwidth of dendritic decoding increases for faster onset dynamics of dendritic spikes (red, dashed). **d** Coherence between somatic input and the logarithm of the event rate (blue) or the logarithm of the firing rate (black). Faster dynamics of dendritic spike does not affect the coherence with event rate (dashed cyan overlay). **e** Information rate for decoding dendritic input from the logarithm of the burst probability (red) and firing rate (black), as a function of the number of cells in the ensemble. **f** Information rate for decoding somatic input from the logarithm of the event rate (blue) and the logarithm of the firing rate (black). Normalization followed from subtracting the mean and dividing by the standard deviation (Z-score).

Materials and Methods). As a result, simulated spike trains display singlets interweaved with short bursts of action potentials. Both types of events appear irregularly in time and are weakly correlated across the population (Fig. S2). In the example illustrated in Fig. 1, the dendritic and somatic inputs were chosen to yield an approximately constant firing rate (Fig. 1c). This illustrates the ambiguity of firing rate responses: the same response could have arisen from a constant somatic input. However, this ambiguity can be resolved since a strong dendritic input is more likely to convert a single spike into a burst. Indeed, the event rate and burst probability qualitatively recover the switching pattern injected in the dendritic and somatic compartment, respectively (Fig. 1d-e). We conclude that active dendrites of TPNs could support the use of event rate and burst probability as distinct channels for encoding somatic and dendritic information streams.

To check this, we characterize the input-output (I-O) function of the ensemble by simulating the population response to short 20-ms current pulses of varying amplitude, delivered simultaneously to all compartments (Fig. 2a-b). Consistent with earlier computational work and *in vitro* recordings of the time-averaged firing rate[14,16,17,44], we found that the ensemble firing rate grows nonlinearly with the somatic input, with a gain that is modulated by concomitant dendritic input (Fig. 2c). Also consistent with the single-cell notion that bursts signal a conjunction of dendritic and somatic inputs[12], the ensemble burst rate in our simulations strongly depends on both somatic and dendritic inputs (Fig. 2d).

The event rate increases nonlinearly with the somatic input (Fig. 2e), but is less modulated by the dendritic input than the firing rate, consistent with an encoding of the somatic input stream. Similarly, burst probability grows with the dendritic input strength with a weak modulation by the concomitant somatic input (Fig. 2f), consistent with our hypothesis that burst probability encodes the dendritic information stream. To quantify encoding quality, we compute a signal-to-noise ratio (SNR_I), which is high for a response that is strongly modulated by the input in one compartment but invariant to input in the other (see SI Data Analysis Methods). We find that both the burst probability and the event rate reached larger SNR_I than either the burst rate or firing rate (maximum $\mathrm{SNR}_I > 250$ for burst probability, and >1000 for the event rate vs $\mathrm{SNR}_I < 10$ for the firing rate and <5 for the burst rate; Fig. S3). Also, the range of input amplitudes with an $\mathrm{SNR}_I > 1$ is broader for burst probability than burst rate (gray regions in Fig. 2e-f). For very high inputs, the clear invariance of somatic and dendritic input in event rate and burst probability breaks down (Fig. S4), because bursts can be triggered by somatic or dendritic input alone and are no longer a conjunctive signal (see Discussion). Therefore multiplexing of dendritic and somatic streams is possible, unless either somatic or dendritic inputs are too strong. The low firing rates and sparse occurrence of bursts typically observed in vivo[5,32,43] are in line with this regime, indicating that TPNs are well-poised to multiplex information.

Multiplexing Rapidly Changing Inputs

Given the need for fast cortical communication[7], we ask if rapidly changing inputs can be reliably represented. To this end, we simulated the response of an ensemble of TPNs receiving two independent input signals, one injected in the dendrites, the other injected in the somata. The time-dependent input fluctuates with equal power in fast and slow frequencies over the 1-100 Hz range (SI Computational Methods). As a first step, we consider the case of a very large ensemble (80 000 cells) in order to minimize finite-size effects. Since the I-O functions obtained from pulse inputs (Fig. 2) are approximately exponential in the moderate input regime, we use the logarithm of the burst probability as an estimate of the dendritic input and the logarithm of the event rate as an estimate of the somatic input. Although crude compared to decoding methods taking into account pairwise correlation and adaptation[45–47], this simple approach recovers accurately both the somatic and dendritic inputs (Fig. 3a-b), with deficits primarily for rapid dendritic input fluctuations. To quantify the encoding quality at different time scales, we calculate the frequency-resolved coherence between the inputs and their estimates. The coherence between dendritic input and its estimate based on the burst probability (Fig. 3c) is close to one for slow input fluctuations, but decreases to zero for rapid input fluctuations. Concurrently, the event rate can decode the somatic input with high accuracy for input frequencies up to 100 Hz (Fig. 3d). In both cases the coherence is at least as high, but typically surpasses the coherence obtained from the classical firing rate code, indicating that burst multiplexing matches but typically surpasses the information contained in the firing rate. To quantify the overall information transferred, we calculate a lower bound for Shannon's mutual information between input and output. This lower bound is formalized by an integral over frequencies of the coherence function $\mathscr{M}$[48] (see *Materials and Methods*), which we refer to as information for brevity. For the input shown in Fig. 3a-b, the firing rate transmitted more than 40 bits/s about the dendritic input (Fig. 3e) and more than 300 bits/s about the somatic input (Fig. 3f). Concurrently, the burst probability transmitted about 200 bits/s (Fig. 3e) while the event rate could transmit more than 400 bits/s about the somatic input (Fig. 3f). Using the information rate for the largest ensemble, we find that, in this simulation, BEM increases overall information by a factor 1.8 compared to the classical rate code. This shows that multiplexing, by preserving information specific to distinct input streams, can be used to transmit more overall information.

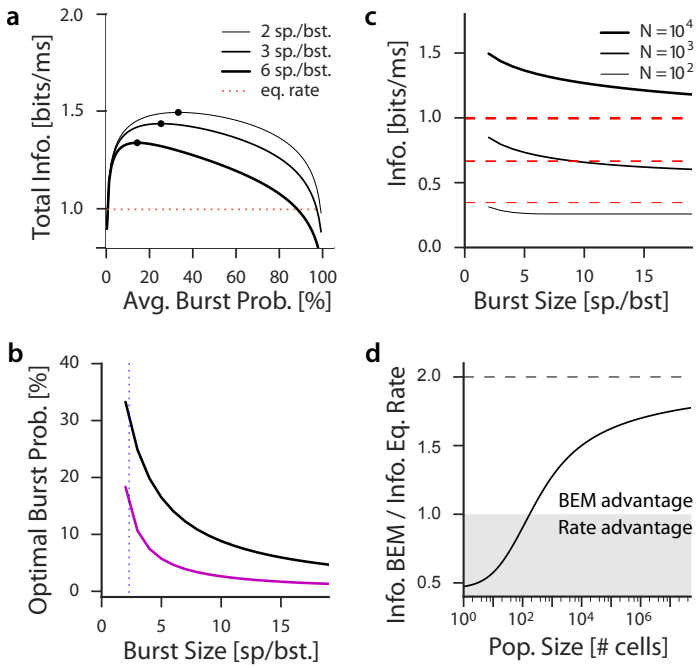

Figure 4 Short and sparse bursts are optimal for multiplexing. **a** Theoretical estimates of total multiplexed information constrained to a fixed total number of spikes is shown (Eqs. S17, S29 and S30 in SI Theoretical Methods with $p = 0.5$, $P = 1$, $N = 10^4$, $W_s = W_d = 100$ Hz and $A_0 = 10$ Hz). The information varies as a function of the stationary burst probability and has a maximum for low burst probability (black circles). The three black lines correspond to three burst sizes (2, 3 and 6 spikes per burst), illustrating that the smallest burst size communicates the greatest amount of information. The information rate for a firing rate code with matched input amplitude and stationary firing rate is shown for comparison (red dashed line, Eq. S12). **b** The stationary burst probability that maximizes information rate decreases as a function of burst size. It reaches 31% for typical burst size (corresponding to an average of 2.3 spikes per burst[32], dotted line) for parameters as in panel a. Considering a smaller dendritic bandwidth $W_d = 0.2W_s$ reduces the optimal burst probability (magenta). **c** The maximum reached by the information rate (solid black curves, N=10^2, 10^3 and 10^4) decreases as a function of burst size. It surpasses information from the firing rate code with matched input amplitude and stationary firing rate (red lines, for corresponding N) for sufficiently large ensembles and for small burst sizes. **d** For matched input amplitude and output rate, the total multiplexed information gain relative to the information rate of the firing rate (Eq. S30 over Eq. S12) asymptotes to two (dashed line). The area where the classical firing rate offers an advantageous coding strategy is shown with shaded gray.

Information-Limiting Factors in Multiplexing

The total amount of information transmitted depends on a variety of extrinsic and intrinsic factors. The main extrinsic factors are the power and the bandwidth of the input signals. High power is manifested in large input changes, which can strongly synchronize cells, and can thus increase the ensemble response. Consistently, the information rates obtained in the previous section depend strongly on our choice of input power. For instance, decreasing the relative power in the dendrites decreases the information rate obtained from the burst probability (Fig. S5). To arrive at a more objective assessment of multiplexing, we derived mathematical expressions for the event and burst information rates at matched input power and total number of spikes. The theoretical analysis is based on information theory and a renewal approximation (SI Theoretical Methods). It allows us to determine how coding depends on the properties and prevalence of bursts as well as the conditions under which multiplexing is advantageous.

Firstly, we find that there is an optimal burstiness, i.e., mean burst probability, for which information transmission is maximized (Fig. 4a). This optimum arises from the fact that rare bursting sacrifices information from the dendritic stream, whereas frequent bursting must sacrifice information from the somatic stream to meet the constraint of total number of spikes. This optimal burstiness depends on the number of spikes in a burst and the bandwidth of the two channels. It decreases with the number of spikes per burst (Fig. 4b), in line with the notion that long bursts convey little information per spike and should hence be used more sparsely. The optimal burstiness further decreases with decreasing dendritic bandwidth (Fig. 4b). The information transmitted decreases with the number of spikes per burst (Fig. 4c), in line with the intuition that the second spike in a burst marks the event as a burst, whereas additional spikes contain no further information. Hence, for neurons with slow dendritic dynamics, BEM performs best when bursts are short and occur rarely, in line with experimental observations[32]. Finally, the preference for short bursts is independent of the number of neurons in the ensemble (Fig. 4c), but a minimal number of neurons is required to transmit more information than a rate code with the same firing rate (Fig. 4c-d). If the somatic and dendritic compartments have the same bandwidth, the total information transmitted by BEM approaches twice the information of a classical rate code, in the limit of very large ensembles (Fig. 4d). In summary, the theoretical analysis suggests that short and sparse bursts in a large ensemble maximize information transmission in burst multiplexing.

Another interesting question is what limits the coherence bandwidth of the burst probability (Fig. 3c)? If it were limited by the dendritic membrane potential dynamics, it could in principle be speeded up by changing membrane properties. If it were limited by the finite duration of bursts, which effectively introduces a long refractory period before the next burst can occur, this could introduce a fundamental speed limit for BEM. The mathematical analysis indicates that the refractory period does not affect the bandwidth of BEM for sufficiently large ensembles (SI Theoretical Methods), consistent with previous theoretical work[49]. Alternatively, the membrane dynamics could limit the bandwidth if the membrane time constant was particularly large in the apical dendrites. In contrast, the high density of the hyperpolarization-activated ion channels[50] contributes to a particularly low dendritic membrane time constant[36]. The other possibility is that the slow onset of dendritic spikes limits the bandwidth[51]. This possibility would be compatible with slow calcium spike onsets observed, arising from the kinetics of calcium ion channels[52]. Therefore, we simulated the response to the same time-dependent input shown in Fig. 3 but with a three-fold increase of the voltage sensitivity for dendritic spikes, to accelerate the onset of dendritic spikes. This single manipulation considerably improved the encoding of high-frequency fluctuations (Fig. 3c-d and Fig. S6). We conclude that one important limitation to burst coding is the slow onset of dendritic spikes.

Decoding: Cortical Microcircuits as a Demultiplexer

For the brain to make use of a multiplexed code, the different streams have to be decodable by neuronal mechanisms. We reason that this could be achieved by short-term plasticity within neuronal microcircuits. To test these ideas, we simulated cell populations receiving excitatory input from TPNs, and studied how the response of these post-synaptic cells depends on the input to TPNs. As a model for short-term plasticity, we used the extended Tsodyks-Markram model[53] with parameters constrained by the reported properties of neocortical connections[37] (see SI Computational Methods). By decreasing the postsynaptic effect of additional spikes in a burst, STD could introduce a selectivity to events, particularly for short bursts and strong depression. Indeed, we find that in a population of cells receiving excitatory TPN inputs, responses correlated slightly more with event rate when STD was present than without short-term plasticity (correlation coefficient 0.995 vs 0.990, Fig. S7a-b). The presence of STD affects the range of SNR_I above one only weakly, but increases the maximum reached by SNR_I considerably (SNR_I reaches 120 with STD, and is below 30 without STD, Fig. S8a-b). STD can hence be interpreted as an event rate decoder. In turn, since TPN event rate encodes the somatic stream (Fig. 2), it is not surprising that we find STD to further suppress the weak dependence on dendritic inputs, while maintaining the selectivity to somatic input (Fig. 5a, b). Hence STD improves the selective decoding of the somatic stream.

To decode the dendritic stream, neurons should compute a quantity similar to the burst probability (Fig. 2d). By increasing the postsynaptic effect of later spikes in a burst[27,28], STF should boost the sensitivity to bursts and hence to the dendritic stream. Indeed, the response of a population receiving facilitating excitatory TPN input was strongly modulated by both the somatic and dendritic streams (Fig. 5c). We then reason that computing burst probability could be achieved by combining burst rate sensitivity with divisive feedforward inhibition from an event rate decoder. Thus, we consider a population receiving facilitating excitatory input from TPNs, combined with divisive feedforward inhibition from an STD-based event rate decoder. We manually adjusted the weights of these connections to increase the post-synaptic effect of dendritic inputs, while decreasing the post-synaptic effect of somatic input. This was achieved with potent excitation and inhibition, a regime associated with divisive inhibition[54,55]. The output rate of this microcircuit displayed a higher correlation with burst probability than for a microcircuit without feedforward inhibition (correlation coefficient 0.951 vs 0.901, Fig. S7c-d). This microcircuit can selectively decode dendritic input (Fig. 5d) with an SNR_I above 1 over a large range of dendritic input amplitudes (Fig. S8d). In the absence of feedforward inhibition, the SNR_I reached one for a very small range of dendritic input amplitudes (Fig. **??**c). Is the presence of STD essential to this operation? In line with the weak dependence of TPN firing rate on dendritic input, we find that the presence of STD in this microcircuit is not essential since decoding of the dendritic stream can also result from STF combined with feedforward inhibition without STD (Fig. S8e-f). We conclude that a microcircuit with STP and feedforward inhibition in a divisive regime can selectively extract different input streams from a multiplexed neural code.

Gain Control of Multiplexed Signals

Our theory suggests that short and sparse bursts are optimal for multiplexing (Fig. 4, SI Theoretical Methods). We now ask if TPNs can be brought into this ideal regime by feedback dendritic inhibition (FDI), that is inhibition triggered by TPN activity and feeding back to the dendrites[12,28]. To this end, we simulated TPNs receiving feedback inhibition from a burst-probability decoder (Fig. 6a). We find that the presence of such FDI reduces the average burst length (Fig. 6b), consistent with similar experimental manipulations in the hippocampus[21]. Also, there is a weaker gain modulation of the firing rate I-O function compared to TPNs without FDI (Fig. 6c). Inhibition from the burst probability decoder

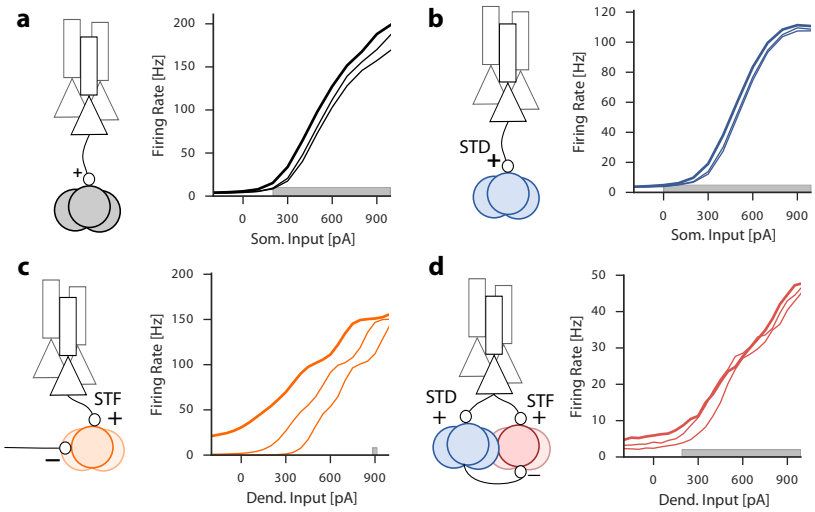

Figure 5 The role of short-term plasticity and feedforward inhibition for separating distinct information streams. **a** Firing rate of a population receiving excitatory input from 4,000 TPNs without STP. The responses are shown as a function of the amplitude of somatic input pulses to the TPNs with concomitant dendritic input pulses with amplitudes 200, 300 and 400 pA. Thicker lines corresponds to the strongest concomitant stimulation. **b** Firing rate of population receiving TPN input with STD. **c** Firing rate of population receiving TPN input with STF and a constant hyperpolarizing current. The responses are shown as a function of dendritic input to the TPNs with concomitant somatic input at 200, 300 and 400 pA. **d** Firing rate of a population stimulated by TPN excitatory input with STF and inhibition from a population receiving STD from TPNs. Gray shade highlights range with $\mathrm{SNR}_I > 1$.

motif does not abolish bursting in the TPNs but reduces both the overall proportion of bursts and the gain of the burst probability I-O function (Fig. 6d). Importantly, FDI does not change the invariance of the burst probability to somatic input, so the multiplexed code is conserved (Fig. 6d). We suggest that this conservation of the code requires that FDI is primarily driven by dendritic input. When divisive feedforward inhibition in the burst-probability decoder is replaced by a constant hyperpolarizing current (Fig. 6e), FDI becomes strongly modulated by somatic input (Fig. S9h). Although bursts remain shorter (Fig. 6f) and more sparse (Fig 6h), and although the gain of the firing rate response is reduced in a very similar fashion (Fig. 6g), the burst probability loses its invariance with respect to somatic input (Fig. 6h). Therefore, FDI from the burst probability decoder motif ensures that bursts are short and sparse and controls the gain of the dendritic signal, while maintaining the suggested multiplexed code.

Discussion

We have introduced a neural code that is able to communicate two streams of information simultaneously in a single neural ensemble. Our simulations indicate that i) this multiplexing is consistent with the properties of active dendrites in TPNs and ii) it can be decoded and improved by select inhibitory microcircuits with short-term plasticity. Based on these findings, we suggest that burst coding may satisfy a need to combine two streams of information without loosing information specific to either. We discuss the experimental evidence supporting this functional view of bursting in terms of the electrophysiology and anatomy of the neocortex, hippocampus and a sensory system.

Our work was motivated by TPNs in layer 5B of the somatosensory cortex, which receive distinct input streams on their somatic and dendritic compartment[56,57] and show dendrite-dependent bursting[12]. Our theory predicts that the input onto these apical dendrites (e.g, by attentional signals[58,59] or feedback signals from motor cortex[56]) should be represented in the propensity of these cells to burst. Consistent with this prediction, burst fraction in somatosensory cortex correlates with the ability of mice to report a light touch[60]. In higher-order cortex, elevated burst fraction is associated with attention in primate frontal cortex[59], which offers an interesting parrallel. However, dendritic signals are not necessarily of top-down character, and the suggested coding scheme could in principle combine arbitrary information streams. Other examples where distinct synaptic pathways target different cortical laminae – and hence probably different neuronal compartments – include inputs from matrix vs. core thalamic cell types[61], from multiple modalities[62] or inputs from callosal vs. local connections[63].

We suggested that a BEM code can be decoded by microcircuits combining STP and inhibition. Candidates to implement this micricircuit are neocortical GABAergic cells. These cells receive input from local TPNs and are known to interconnect into specific microcircuits. Consistent with the circuit motifs described in Fig. 5, cortical somatostatin-positive (SOM) cells typically receive facilitating inputs from TPNs[30,53,64], while parvalbumin-positive (PV) cells and vaso-intestinal peptide-positive (VIP) cells typically receive depressing TPN input[30,53,64]. Compatible with the burst probability decoder in Fig. 5d, feedforward inhibition onto SOM cells arises from either PV or VIP cells[34,35]. Interestingly, the large membrane time constant of SOM cells[28,64] is consistent with a burst code that is restricted to slowly changing signals by slow dendritic onset dynamics (Fig. 3). A sub-type of SOM cells, the Martinotti cells, inhibit specifically the dendrites[65] and act as a powerful control of dendritic spikes[12,66,67], consistent with the motif used in Fig. 6a. This suggests that Martinotti cells are well-poised to encode burst probability. This role may come in addition to their function in pathway gating[25] and surround suppression[68,69]. Whether PV or VIP cells encode event rate remains to be seen, particularly given that VIP cells receive direct top-down inputs[70,71]. Connection motifs that could decode multiplexed codes are not restricted to neurons in the vicinity of TPNs. We hypothesize that

such circuits are beneficial wherever TPN outputs need to be interpreted. For example, long-range connections from the cortex to the thalamus show a combination of STF and feedforward inhibition[72].

In CA1 pyramidal cells of the hippocampus, bursts can also be generated by the conjunction of somatic and dendritic input, a mechanism similar to bursting in TPNs. The time-averaged burst probability has been analyzed in CA1 pyramidal neurons in vivo[22,73]. Compatible with our simulations, trial-averaged burst fraction of CA1 pyramidal cells locked to the same phase of the theta rhythm as the population of cells projecting to the apical dendrites, while the firing rate locked to the same phase of the theta rhythm as the cells projecting to the proximal dendrites[22]. The observation that the burst fraction increases in the surround of the place field[22,73] also indicates that additional information can be gained by assuming a neural code that distinguishes between spikes and bursts.

In other systems, the hypothesis that bursts convey distinct information from single spikes has long been surmised[74,75], and it is possible that BEM also applies to non-mammalian systems. Bursting in the pyramidal neurons of the electrosensory lateral lobe (ELL) of weakly electric fish arises from a dendrite-dependent boost of an isolated back-propagating action potential[40,41]. These neurons also combine two distinct types of information: their apical dendrites receive feedback from higher order areas, while the basal dendrites integrate information from the electroreceptors[40,76,77]. Trial-averaged responses show independent modulation of burst fraction and firing rate[76] and the burst response depends strongly on higher-order feedback[77]. While these observations suggest that burst coding is an essential mechanism of information processing in hierarchical structures, our work further suggests that bursts allow multiplexing of bottom-up and top-down streams, potentially enabling particular forms of predictive coding or reward learning[24,78,79].

The ensemble code we have described relies on the assumption that spikes are probabilistically converted into bursts independently across neurons. Dendrites should hence be in an asynchronous state with weak pairwise correlations. This asynchronous state allows a rapid[80] and efficient[81] encoding. In our simulations, the asynchronous state was mimmicked by a substantial background noise that effectively desynchronized and linearized the responses of both somatic and dendritic compartments. A physiological basis for this background noise could lie in a state of balanced excitation and inhibition, which is known to favor pairwise decorrelation[2,5] and could be supported by homeostatic inhibitory synaptic plasticity[82].

In BEM, the semantic links "burst probability – dendritic inputs" and "event rate – somatic input" rely specifically on the *conjunctive* bursting mechanism of TPNs, in which dendritic input converts somatically generated single spikes into bursts[12]. Different bursting mechanisms could alter these semantic links, while maintaining a multiplexed code. A simple example would be a non-conjunctive bursting mechanism, in which dendritic inputs alone can trigger regenerative dendritic potentials, which in turn generate somatic bursts. In this case, dendritic inputs could be semantically linked to burst rate rather than burst probability. Given that a variety of different bursting mechanisms has been reported[12,13,15,40], we are lead to a central prediction of the BEM hypothesis. To extract and transmit a desired combination of the two input streams, the circuits that decode this signal have to match the properties of the cellular encoder. Burst ensemble coding hence requires a synergistic coordination among single cell bursting mechanisms, the morphological targets of different input streams on these cells, and neuronal circuit motifs. Whether hallmarks of such a coordination can be found in different neuronal systems, and how this synergy is established and maintained by synaptic, neuronal and circuit plasticity remains an open question.

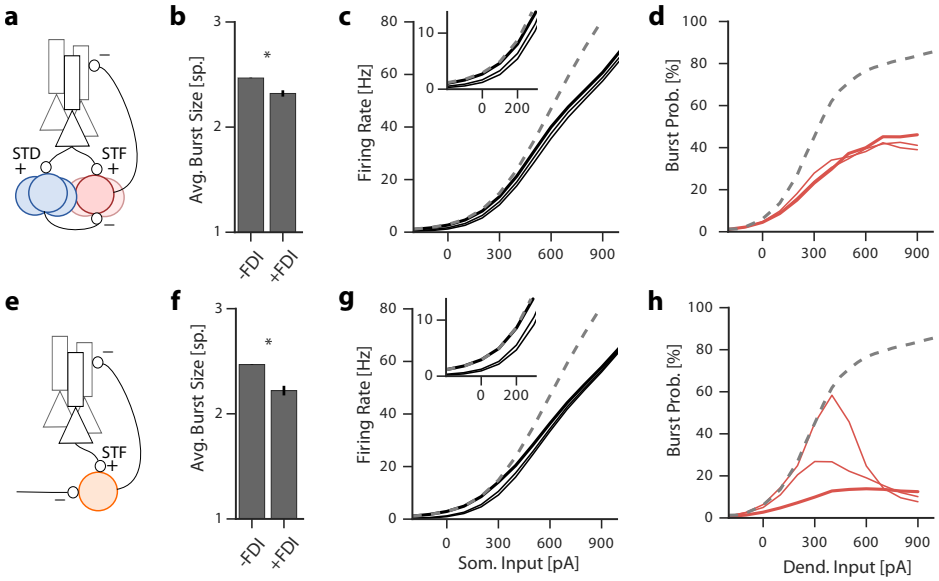

Figure 6 Dendritic feedback inhibition controls multiplexing gain. **a** Schematic representation of the simulated network. **b** Burst size averaged across simulated input conditions with and without feedback dendritic inhibition (FDI). **c** Dependence of TPN firing rate on somatic input for three different amplitudes of dendritic input pulses (0, 200 and 400 pA). **d** Dependence of burst probability on the dendritic input for three different somatic input amplitudes (0, 200 and 400 pA). The thicker line shows the response with the strongest somatic input. **e**-**h** As above, but replacing the feedforward inhibition by an hyperpolarizing current (430 pA). In this case, the burst probability associated to mild dendritic input is decreased by somatic input (**h**). Star indicate significant difference (Welch's test $p<0.0001$). Dashed line shows response in the absence of FDI (corresponding to thick lines in Fig. 2).

Materials and Methods

Network simulations

The network consists of four types of units: pyramidal-cell basal bodies, pyramidal-cell distal dendrites and inhibitory cells from population a receiving STF and b receiving STD. We used the lower case letters s, d, a and b to label the different units, respectively. Somatic dynamics follow generalized integrate-and-fire dynamics described by a membrane potential u and a generic recovery variable w to account for subthreshold-activated ion channels and spike-triggered adaptation[1]. For the ith unit in population x we used

$$\frac{d}{dt}u_i^{(x)} = -\frac{u_i^{(x)} - E_L}{\tau_x} + \frac{g_x f(u_i^{(\mathsf{d})}) + c_x K(t - \hat{t}_i^{(\mathsf{s})}) + I_i^{(x)} + w_i^{(x)}}{C_x} \tag{1}$$

$$\frac{d}{dt}w_i^{(x)} = -w_i^{(x)}/\tau_w^{(x)} + a_w^{(x)}\left(u_i^{(x)} - E_L\right)/\tau_w^{(x)} + b_w^{(x)} S_i^{(x)} \tag{2}$$

where E_L is the reversal potential, C_x the capacitance, $a_w^{(x)}$ the strength of subthreshold coupling, $b_w^{(x)}$ the strength of spike-triggered adaptation, $\tau_w^{(x)}$ the time scale of the recovery variable, $\tau_u^{(x)}$ the time scale of the membrane potential and $\hat{t}_i^{(\mathsf{s})}$ the somatic spike times of cell i (see Sl Computational Methods for parameter values). An additional term controlled by g_x (Eq. 1) models the regenerative activity in the dendrites as described below, but is absent from inhibitory cells ($g_\mathsf{a} = g_\mathsf{b} = 0$). Also, an additional term controlled by c_x and the kernel K (see SI Computational Methods) models how the last action potential at $t_i^{(s)}$ is back propagating from the soma in the dendrites, and is absent from all other units (c_s,c_a,c_b = 0). When units s, a and b reach a threshold at V_T the membrane potential is reset to the reversal potential after an absolute refractory period of 3 ms and a spike is added to the spike train $S_i^{(x)}$ in the form of a sum of Dirac functions.

The dendritic compartment has nonlinear dynamics dictated by the sigmoidal function f to model the nonlinear activation of calcium channels[36]. This current propagates to the somatic unit such that g_s controls the somatic effect of forward calcium spike propagation. In the dendritic compartment, the parameter g_d controls the potency of local regenerative activity. The dendritic recovery variable controls both the duration of the calcium spike consistent with potassium currents[20,83] and resonating subthreshold dynamics consistent with h-current[50]. Note that the differential equations are similar to those used to model NMDA spikes[84], but the strong and relatively fast recovery variable ensures that the calcium spikes have shorter durations (10-40 ms). Membrane time constants were chosen to the values found in vivo[64] (see SI Computational Methods for parameter values).

Each unit receives a combination of synaptic input, external input and background noise (see SI Computational Methods). Synapses were modeled as exponentially decaying changes in conductance. Connection probability was chosen to 0.2 for excitatory connections and one for inhibitory connections consistent with experimental observations[64,85]. Background noise was modeled as a time-dependent Ornstein-Uhlenbeck process independently drawn for each unit. We chose the amplitude of background fluctuations to be such that the standard deviation of membrane potential fluctuations is around 6 mV as observed in V1 L2-3 pyramidal neurons[43]. To model short-term plasticity, we used the extended Tsodyks-Markram model[37,53] with parameters consistent with experimental calibrations *in vitro*[37] (see SI Computational Methods).

Statistical Analysis

Bursts are defined as a set of spikes followed or preceded by an interspike interval smaller than 16 ms. Mutual information between the population-averaged quantities (firing rate, event rate or burst probability) and somatic or

dendritic membrane potential was quantified with Shannon's information for the Gaussian channel[48]

$$\mathscr{M} = -\int \log_2 (1 - C(\omega))\, d\omega \tag{3}$$

where $C(\omega)$ is the coherence between quantity X and Y. The integral was limited between 0 and 100 Hz and the power spectra was calculated with windows of 409 ms.

1. Gerstner, W., Kistler, W., Naud, R. & Paninski, L. *Neuronal Dynamics* (Cambridge University Press, Cambridge, 2014).

2. van Vreeswijk, C. & Sompolinsky, H. Chaos in neuronal networks with balanced excitatory and inhibitory activity. *Science* **274**, 1724–1726 (1996).

3. Banerjee, A., Seriès, P. & Pouget, A. Dynamical constraints on using precise spike timing to compute in recurrent cortical networks. *Neural Comput.* **20**, 974–993 (2008).

4. London, M., Roth, A., Beeren, L., Häusser, M. & Latham, P. E. Sensitivity to perturbations in vivo implies high noise and suggests rate coding in cortex. *Nature* **466**, 123–127 (2010).

5. Renart, A. *et al.* The asynchronous state in cortical circuits. *Science* **327**, 587–90 (2010).

6. Pozzorini, C., Naud, R., Mensi, S. & Gerstner, W. Temporal whitening by power-law adaptation in neocortical neurons. *Nat Neurosci* **16**, 942–948 (2013).

7. Thorpe, S., Fize, D. & Marlot, C. Speed of processing in the human visual system. *Nature* **381**, 520–522 (1996).

8. Knight, B. W. Dynamics of encoding in a population of neurons. *J. Gen. Physiology* **59**, 734–766 (1972).

9. Strong, S. P., Koberle, R., de Ruyter van Steveninck, R. R. & Bialek, W. Entropy and information in neural spike trains. *Phys. Rev. Lett.* **80**, 197–200 (1998).

10. Kayser, C., Montemurro, M., Logothetis, N. & Panzeri, S. Spike-phase coding boosts and stabilizes information carried by spatial and temporal spike patterns. *Neuron* **61**, 597–608 (2009).

11. Panzeri, S., Brunel, N., Logothetis, N. K. & Kayser, C. Sensory neural codes using multiplexed temporal scales. *Trends Neurosci.* **33**, 111–120 (2010).

12. Larkum, M., Zhu, J. & Sakmann, B. A new cellular mechanism for coupling inputs arriving at different cortical layers. *Nature* **398**, 338–341 (1999).

13. Brumberg, J. C., Nowak, L. G. & McCormick, D. A. Ionic mechanisms underlying repetitive high-frequency burst firing in supragranular cortical neurons. *J. Neurosci.* **20**, 4829–4843 (2000).

14. Larkum, M. E., Senn, W. & Luscher, H.-R. Top-down dendritic input increases the gain of layer 5 pyramidal neurons. *Cereb. Cortex* **14**, 1059–1070 (2004).

15. Izhikevich, E. M. *Dynamical systems in neuroscience : the geometry of excitability and bursting* (MIT Press, Cambridge, Mass., 2007).

16. Hay, E. & Segev, I. Dendritic excitability and gain control in recurrent cortical microcircuits. *Cereb. Cortex* bhu200 (2014).

17. Shai, A. S., Anastassiou, C. A., Larkum, M. E. & Koch, C. Physiology of layer 5 pyramidal neurons in mouse primary visual cortex: coincidence detection through bursting. *PLoS Comput Biol* **11**, e1004090 (2015).

18. Xu, N.-l. *et al.* Nonlinear dendritic integration of sensory and motor input during an active sensing task. *Nature* **492**, 247–251 (2012).

19. Larkum, M. A cellular mechanism for cortical associations: an organizing principle for the cerebral cortex. *Trends Neurosci.* **36**, 141–151 (2013).

20. Harnett, M. T., Xu, N.-L., Magee, J. C. & Williams, S. R. Potassium channels control the interaction between active dendritic integration compartments in layer 5 cortical pyramidal neurons. *Neuron* **79**, 516–529 (2013).

21. Royer, S. *et al.* Control of timing, rate and bursts of hippocampal place cells by dendritic and somatic inhibition. *Nat. Neurosci.* **15**, 769–775 (2012).

22. Bittner, K. C. *et al.* Conjunctive input processing drives feature selectivity in hippocampal ca1 neurons. *Nat. Neurosci.* **18**, 1133–1142 (2015).

23. Poirazi, P. & Mel, B. W. Impact of active dendrites and structural plasticity on the memory capacity of neural tissue. *Neuron* **29**, 779–96 (2001).

24. Urbanczik, R. & Senn, W. Learning by the dendritic prediction of somatic spiking. *Neuron* **81**, 521–528 (2014).

25. Yang, G. R., Murray, J. D. & Wang, X.-J. A dendritic disinhibitory circuit mechanism for pathway-specific gating. *Nature Commun.* **7** (2016).

26. Mel, B. W. Toward a simplified model of an active dendritic tree. *Dendrites* 465 (2016).

27. Markram, H., Wu, Y. & Tosdyks, M. Differential signaling via the same axon of neocortical pyramidal neurons. *Proc. Natl. Acad. Sci. USA* **95**, 5323–5328 (1998).

28. Silberberg, G. & Markram, H. Disynaptic inhibition between neocortical pyramidal cells mediated by martinotti cells. *Neuron* **53**, 735–746 (2007).

29. Berger, T. K., Silberberg, G., Perin, R. & Markram, H. Brief bursts self-inhibit and correlate the pyramidal network. *PLoS Biol.* **8**, e1000473 (2010).

30. Reyes, A. *et al.* Target-cell-specific facilitation and depression in neocortical circuits. *Nat. Neurosci.* **1**, 279–285 (1998).

31. Pockberger, H. Electrophysiological and morphological properties of rat motor cortex neurons in vivo. *Brain Res.* **539**, 181–190 (1991).

32. De Kock, C. & Sakmann, B. High frequency action potential bursts ($>$ 100 hz) in l2/3 and l5b thick tufted neurons in anaesthetized and awake rat primary somatosensory cortex. *J. Physiol.* **586**, 3353–3364 (2008).

33. Urban-Ciecko, J. & Barth, A. L. Somatostatin-expressing neurons in cortical networks. *Nat Rev Neurosci* **16**, 401–409 (2016).

34. Pfeffer, C. K., Xue, M., He, M., Huang, Z. J. & Scanziani, M. Inhibition of inhibition in visual cortex: the logic of connections between molecularly distinct interneurons. *Nat. Neurosci.* **16**, 1068–1076 (2013).

35. Jiang, X. *et al.* Response to comment on ?principles of connectivity among morphologically defined cell types in adult neocortex? *Science* **353**, 1108–1108 (2016).

36. Naud, R., Bathellier, B. & Gerstner, W. Spike-timing prediction in cortical neurons with active dendrites. *Front. Comput. Neurosci.* **8**, 90 (2014).

37. Costa, R. P., Sjöström, P. J. & Van Rossum, M. C. Probabilistic inference of short-term synaptic plasticity in neocortical microcircuits. *Front. Comput. Neurosci.* **7** (2013).

38. Deschênes, M., Paradis, M., Roy, J. & Steriade, M. Electrophysiology of neurons of lateral thalamic nuclei in cat: resting properties and burst discharges. *J. Neurophys.* **51**, 1196–1219 (1984).

39. Magee, J. C. & Carruth, M. Dendritic voltage-gated ion channels regulate the action potential firing mode of hippocampal ca1 pyramidal neurons. *J. Neurophys.* **82**, 1895–1901 (1999).

40. Oswald, A., Chacron, M., Doiron, B., Bastian, J. & Maler, L. Parallel processing of sensory input by bursts and isolated spikes. *Journal of Neuroscience* **24**, 4351–4362 (2004).

41. Bastian, J. & Nguyenkim, J. Dendritic modulation of burst-like firing in sensory neurons. *Journal of Neurophysiology* **85**, 10–22 (2001).

42. Larkum, M. E., Kaiser, K. & Sakmann, B. Calcium electrogenesis in distal apical dendrites of layer 5 pyramidal cells at a critical frequency of back-propagating action potentials. *Proc. Natl. Acad. Sci. USA* **96**, 14600–14604 (1999).

43. Polack, P.-O., Friedman, J. & Golshani, P. Cellular mechanisms of brain state-dependent gain modulation in visual cortex. *Nat. Neurosci.* **16**, 1331–1339 (2013).

44. Giugliano, M., La Camera, G., Fusi, S. & Senn, W. The response of cortical neurons to in vivo-like input current: theory and experiment: Ii. time-varying and spatially distributed inputs. *Biol. Cybern.* **99**, 303–318 (2008).

45. Bialek, W., Rieke, F., de Ruyter Van Steveninck, R. & Warland, D. Reading a neural code. *Science* **252**, 1854–1857 (1991).

46. Pillow, J. *et al.* Spatio-temporal correlations and visual signalling in a complete neuronal population. *Nature* **454**, 995–999 (2008).

47. Naud, R. & Gerstner, W. Coding and decoding with adapting neurons: A population approach to the peri-stimulus time histogram. *PLOS Comput. Biol.* **8**, e1002711 (2012).

48. Rieke, F., Warland, D., de Ruyter van Steveninck, R. & Bialek, W. *Spikes - Exploring the neural code* (MIT Press, Cambridge, MA, 1996).

49. Deger, M., Schwalger, T., Naud, R. & Gerstner, W. Fluctuations and information filtering in coupled populations of spiking neurons with adaptation. *Phys. Rev. E* **90**, 062704 (2014).

50. Kole, M. H. P., Hallermann, S. & Stuart, G. J. Single ih channels in pyramidal neuron dendrites: properties, distribution, and impact on action potential output. *J. Neurosci.* **26**, 1677–87 (2006).

51. Wei, W. & Wolf, F. Spike onset dynamics and response speed in neuronal populations. *Phys. Rev. Lett.* **106**, 088102 (2011).

52. Pérez-Garci, E., Gassmann, M., Bettler, B. & Larkum, M. The gabab1b isoform mediates long-lasting inhibition of dendritic ca2+ spikes in layer 5 somatosensory pyramidal neurons. *Neuron* **50**, 603–616 (2006).

53. Markram, H., Wang, Y. & Tsodyks, M. Differential signaling via the same axon of neocortical pyramidal neurons. *Proc. Nal. Acad. Sci. USA* **95**, 5323–5328 (1998).

54. Doiron, B., Longtin, A., Berman, N. & Maler, L. Subtractive and divisive inhibition: effect of voltage-dependent inhibitory conductances and noise. *Neural Comput.* **13**, 227–248 (2001).

55. Murphy, B. K. & Miller, K. D. Multiplicative gain changes are induced by excitation or inhibition alone. *J. Neurosci.* **23**, 10040–10051 (2003).

56. Petreanu, L., Mao, T., Sternson, S. M. & Svoboda, K. The subcellular organization of neocortical excitatory connections. *Nature* **457**, 1142–5 (2009).

57. Xu, H., Jeong, H.-Y., Tremblay, R. & Rudy, B. Neocortical somatostatin-expressing gabaergic interneurons disinhibit the thalamorecipient layer 4. *Neuron* **77**, 155–167 (2013).

58. Van Kerkoerle, T., Self, M. W. & Roelfsema, P. R. Layer-specificity in the effects of attention and working memory on activity in primary visual cortex. *Nat. Commun.* **8**, 13804 (2017).

59. Womelsdorf, T., Ardid, S., Everling, S. & Valiante, T. A. Burst firing synchronizes prefrontal and anterior cingulate cortex during attentional control. *Current Biology* **24**, 2613–2621 (2014).

60. Takahashi, N., Oertner, T. G., Hegemann, P. & Larkum, M. E. Active cortical dendrites modulate perception. *Science* **354**, 1587–1590 (2016).

61. Jones, E. G. The thalamic matrix and thalamocortical synchrony. *Trends Neurosci.* **24**, 595–601 (2001).

62. Schroeder, C. E. & Foxe, J. J. The timing and laminar profile of converging inputs to multisensory areas of the macaque neocortex. *Cogn. Brain Res.* **14**, 187–198 (2002).

63. Palmer, L. M. *et al.* Nmda spikes enhance action potential generation during sensory input. *Nat. Neurosci.* **17**, 383–390 (2014).

64. Pala, A. & Petersen, C. C. In vivo measurement of cell-type-specific synaptic connectivity and synaptic transmission in layer 2/3 mouse barrel cortex. *Neuron* **85**, 68–75 (2015).

65. Markram, H. *et al.* Interneurons of the neocortical inhibitory system. *Nat Rev Neurosci* **5**, 793–807 (2004).

66. Gidon, A. & Segev, I. Principles governing the operation of synaptic inhibition in dendrites. *Neuron* **75**, 330–341 (2012).

67. Murayama, M. *et al.* Dendritic encoding of sensory stimuli controlled by deep cortical interneurons. *Nature* **457**, 1137–1141 (2009).

68. Adesnik, H., Bruns, W., Taniguchi, H., Huang, Z. J. & Scanziani, M. A neural circuit for spatial summation in visual cortex. *Nature* **490**, 226–231 (2012).

69. Litwin-Kumar, A., Rosenbaum, R. & Doiron, B. Inhibitory stabilization and visual coding in cortical circuits with multiple interneuron subtypes. *Journal of Neurophysiology* **115**, 1399–1409 (2016).

70. Lee, S., Kruglikov, I., Huang, Z. J., Fishell, G. & Rudy, B. A disinhibitory circuit mediates motor integration in the somatosensory cortex. *Nat. Neurosci.* **16**, 1662–1670 (2013).

71. Pi, H.-J. *et al.* Cortical interneurons that specialize in disinhibitory control. *Nature* **503**, 521–524 (2013).

72. Cruikshank, S. J., Urabe, H., Nurmikko, A. V. & Connors, B. W. Pathway-specific feedforward circuits between thalamus and neocortex revealed by selective optical stimulation of axons. *Neuron* **65**, 230–245 (2010).

73. Harris, K. D., Hirase, H., Leinekugel, X., Henze, D. A. & Buzsáki, G. Temporal interaction between single spikes and complex spike bursts in hippocampal pyramidal cells. *Neuron* **32**, 141–149 (2001).

74. Crick, F. Function of the thalamic reticular complex: the searchlight hypothesis. *Proc. Natl. Acad. Sci. USA* **81**, 4586–4590 (1984).

75. Krahe, R. & Gabbiani, F. Burst firing in sensory systems. *Nat. Rev. Neurosci.* **5**, 13–23 (2004).

76. Clarke, S. E., Longtin, A. & Maler, L. A neural code for looming and receding motion is distributed over a population of electrosensory on and off contrast cells. *J. Neurosci.* **34**, 5583–5594 (2014).

77. Clarke, S. E. & Maler, L. Feedback synthesizes neural codes for motion. *Curr. Biol.* **27**, 1356–1361 (2017).

78. Bastos, A. M. *et al.* Canonical microcircuits for predictive coding. *Neuron* **76**, 695–711 (2012).

79. Scellier, B. & Bengio, Y. Towards a biologically plausible backprop. *arXiv preprint arXiv:1602.05179* (2016).

80. Gerstner, W. Population dynamics of spiking neurons: Fast transients, asynchronous states, and locking. *Neural Comput.* **12**, 43–89 (2000).

81. Sompolinsky, H., Yoon, H., Kang, K. & Shamir, M. Population coding in neuronal systems with correlated noise. *Phys. Rev. E* **64**, 051904 (2001).

82. Vogels, T. P., Sprekeler, H., Zenke, F., Clopath, C. & Gerstner, W. Inhibitory plasticity balances excitation and inhibition in sensory pathways and memory networks. *Science* **334**, 1569–1573 (2011).

83. Cai, X. *et al.* Unique roles of sk and kv4. 2 potassium channels in dendritic integration. *Neuron* **44**, 351–364 (2004).

84. Major, G., Polsky, A., Denk, W., Schiller, J. & Tank, D. W. Spatiotemporally graded nmda spike/plateau potentials in basal dendrites of neocortical pyramidal neurons. *J Neurophysiol* **99**, 2584–601 (2008).

85. Fino, E. & Yuste, R. Dense inhibitory connectivity in neocortex. *Neuron* **69**, 1188–1203 (2011).